

# Structure and Stability of Molecular Crystals with Many-Body Dispersion-Inclusive Density Functional Tight Binding

Majid Mortazavi,<sup>†</sup> Jan Gerit Brandenburg,<sup>‡,§,||</sup> Reinhard J. Maurer,<sup>\*,#</sup> and Alexandre Tkatchenko<sup>\*,∇,†</sup>

<sup>†</sup>Fritz-Haber-Institut der Max-Planck-Gesellschaft, Faradayweg 4-6, 14195 Berlin, Germany

<sup>‡</sup>Department of Chemistry, University College London, 20 Gordon Street, WC1H 0AJ London, United Kingdom

<sup>§</sup>London Centre for Nanotechnology, University College London, 17-19 Gordon Street, WC1H 0AJ London, United Kingdom

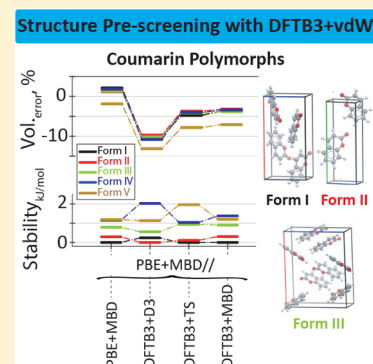
<sup>||</sup>Thomas Young Centre, University College London, Gower Street, WC1E 6BT London, United Kingdom

<sup>#</sup>Department of Chemistry and Centre for Scientific Computing, University of Warwick, Gibbet Hill Road, Coventry CV4 7AL, United Kingdom

<sup>∇</sup>Physics and Materials Science Research Unit, University of Luxembourg, L-1511, Luxembourg

## Supporting Information

**ABSTRACT:** Accurate prediction of structure and stability of molecular crystals is crucial in materials science and requires reliable modeling of long-range dispersion interactions. Semiempirical electronic structure methods are computationally more efficient than their ab initio counterparts, allowing structure sampling with significant speedups. We combine the Tkatchenko–Scheffler van der Waals method (TS) and the many-body dispersion method (MBD) with third-order density functional tight-binding (DFTB3) via a charge population-based method. We find an overall good performance for the X23 benchmark database of molecular crystals, despite an underestimation of crystal volume that can be traced to the DFTB parametrization. We achieve accurate lattice energy predictions with DFT+MBD energetics on top of vdW-inclusive DFTB3 structures, resulting in a speedup of up to 3000 times compared with a full DFT treatment. This suggests that vdW-inclusive DFTB3 can serve as a viable structural prescreening tool in crystal structure prediction.



## INTRODUCTION

Stability and structure prediction of molecular materials from first-principles electronic structure calculations bears significance to a wide range of problems ranging from pharmaceutical activity of drugs to optical properties of modern organic materials.<sup>1–3</sup> The rugged and complex energy landscapes of molecular crystals give rise to the phenomenon of polymorphism—the ability of molecules to form different crystal-packing motifs—which is a crucial aspect in drug design, food chemistry, and organic semiconductor materials.<sup>4–7</sup> Polymorphic materials exhibit many energetically close-lying minima, which can easily coexist and transform into each other at time scales that are inaccessible by conventional molecular dynamic simulations. Rigorous computational polymorph screening followed by correct stability ranking is therefore a crucial aspect for molecular crystal structure prediction (CSP).<sup>8–11</sup>

In recent years, DFT methods have become more reliable in predicting and ranking polymorphic systems due to the incorporation of efficient dispersion correction methods that,<sup>9,12–15</sup> at the same time, ensure computational feasibility.<sup>10,16–19</sup> In particular, the inclusion of beyond-pairwise dispersion interactions through the many-body dispersion (MBD) method coupled to semilocal DFT functionals has proven to be successful in this context.<sup>10,15,20</sup> To address larger

length and time scales and more efficient structure prediction, several approximate electronic structure methods have been highly successful including semiempirical quantum chemical methods such as AM1, PM7, or the DFT-based density-functional tight binding (DFTB).<sup>21–23</sup> DFTB has been significantly improved recently, particularly in its description of charge polarization via third-order charge fluctuation corrections (DFTB3)<sup>24,25</sup> or its description of hydrogen bonding.<sup>26</sup> Nevertheless, several shortcomings still persist that prohibit its use as standard tool in structure and stability prediction for molecular crystals.<sup>22,27</sup> The most detrimental shortcoming is the lack of long-range dispersion inherited from (semi)-local DFT with which DFTB models are parametrized,<sup>28</sup> although early works augmented DFTB with an empirical correction potential.<sup>29</sup>

Many recent works have established pairwise dispersion corrections including the D3 and the dDMC methods parametrized for DFTB3.<sup>30,31</sup> Pre-calculated and tabulated  $C_6$  (dipole–dipole) coefficients are used to calculate pairwise-additive dispersion energies in these methods. The  $C_6$

Received: December 6, 2017

Accepted: January 3, 2018

Published: January 3, 2018

coefficients in D3 are environment-dependent via a fractional coordination number and thus do not directly depend on the electronic structure.<sup>32</sup> The Tkatchenko–Scheffler methods, for example, TS and MBD, use a Hirshfeld partitioning of the electron density, which provides a rescaling of free-atom reference dispersion parameters according to the local atomic environment.<sup>15,33,34</sup> All of those methods have been proven to be highly accurate in capturing long-range dispersion interactions for a variety of systems with their strengths in different types of materials. Stöhr et al. have recently proposed a method to replace the Hirshfeld density-partitioning scheme with a charge population analysis that directly correlates atom-wise dispersion coefficients and a given Hamiltonian in local basis representation.<sup>35</sup> This enables the incorporation of the TS and MBD methods into DFTB and other semiempirical methods, where a real-space representation of the electron density is not directly available. Preliminary benchmarks of lattice and interaction energies have shown that these vdW-corrected DFT and DFTB models give comparable accuracy with the original TS/MBD implementation when based on predetermined molecular geometries for a broad range of systems. This suggests the potential application of DFTB+vdW methods in reliable and efficient structural prescreening of molecular CSP, as sketched in Figure 1.

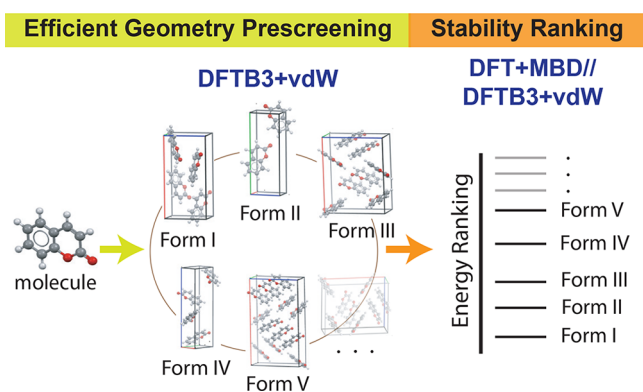


**Figure 1.** Crystal structure prediction: The prescreening step via efficient semiempirical DFTB3+vdW method (left) prior to accurate stability ranking via DFT+vdW single-point energy on top of DFTB3+vdW geometries (right). Inset (middle) shows the molecular models of the five experimentally observed coumarin polymorphs.

Motivated by this finding and a recently developed implementation of analytical atomic forces in the MBD method,<sup>36,37</sup> in this work, we couple the state-of-the-art DFTB3 parameter set 3ob for organic molecules<sup>25,27</sup> with the TS and MBD methods for dispersion energy by calculating optimally tuned range-separation parameters, enabling the standardized use of DFTB3(3ob)+TS/MBD. Thus we present for the first time a modern semiempirical Hamiltonian that includes vdW interactions to all atomic dipole orders based on anisotropic polarizabilities. We perform full geometry optimizations for the X23 benchmark database of organic crystals and demonstrate the large-scale applicability of the method on the example of the polymorphic molecular crystals such as coumarin and a flexible pharmaceutical molecule 2-((4-(3,4-dichlorophenethyl)phenyl)amino)benzoic acid (C<sub>21</sub>H<sub>17</sub>Cl<sub>2</sub>NO<sub>2</sub>) from the sixth CSP blind test organized by the Cambridge Crystallographic Data Centre (CCDC). We find that vdW-inclusive DFTB3, in particular, DFTB3+TS/

MBD, are viable methods for an accurate description of molecular crystal structure, and we identify challenges for the current 3ob parametrization of DFTB3.

The X23 benchmark data set represents a mixture of molecular crystals dominated by hydrogen, vdW, and combined hydrogen–vdW bonding interactions.<sup>38,39</sup> We first analyze the quality of the dispersion-corrected DFTB3 geometries in terms of crystal volume and calculated root-mean-squared deviation (RMSD) for the X23 data set. The comparison was made with respect to the experimental crystal structures determined at the lowest possible temperature.<sup>39</sup> The crystal volume evaluates the overall crystal lattice description, whereas the RMSD provides a more detailed evaluation of molecular orientation and alignment within the corresponding molecular crystal. The lattice energies were compared against experimental measurements (via back-corrected experimental sublimation enthalpies).<sup>10,39</sup> Revised experimental or high-level calculation data was used for benzene,<sup>40</sup> naphthalene,<sup>41</sup> and cytosine.<sup>42</sup> We also made sure the lowest energy conformer of gas-phase (isolated molecule) was selected for calculations of 0 K lattice energies,<sup>39</sup> and special attention was given to cytosine,<sup>43</sup> oxalic acid,<sup>44</sup> succinic acid,<sup>45</sup> and urea<sup>46</sup> due to their conformational flexibility. A summary of statistics of the volumes, lattice energies, and RMSD of the X23 data set is given in Table 1, with more details to be found in Figures S1 and S2 and Tables S1 and S2 in the Supporting Information (SI).

The three studied PBE+vdW methods are quite comparable in describing the crystal volumes with overall MARE values ranging from 1.8 to 2.6%, with PBE+MBD yielding the best performance when compared with experiment. PBE+D3

**Table 1.** Mean Absolute Error (MAE), Mean Error (ME), and Mean Absolute Relative Error (MARE) in Volumes and Lattice Energies of vdW-Inclusive DFT(B3) Methods on the X23 Dataset with Respect to the Reference Experimental Values. Mean RMSD of the Dataset with Respect to Experimental Structures Are Also Listed.

method	geometry			RMSD (Å)
	volumes			
	MAE (Å <sup>3</sup> )	ME (%)	MARE (%)	
PBE+D3	6.4	0.02	2.0	0.18
PBE+TS	8.3	−1.12	2.6	0.12
PBE+MBD	5.5	−0.16	1.8	0.12
DFTB3+D3	36.6	−11.23	11.2	0.26
DFTB3+TS	17.8	−5.52	5.6	0.17
DFTB3+MBD	14.8	−4.07	5.0	0.17
vdW method	lattice energies			MARE (%)
	MAE (kJ mol <sup>−1</sup> )	ME (%)	MARE (%)	
PBE+vdW//PBE+vdW				
D3	4.0	1.7	5.6	
TS	14.0	16.2	17.5	
MBD	4.8	3.2	6.4	
PBE+vdW//DFTB3+vdW				
D3	7.0	−7.4	8.6	
TS	12.8	12.0	16.2	
MBD	4.3	−1.1	5.5	
PBE+MBD//DFTB3+vdW				
D3	6.7	−6.0	8.7	
TS	4.8	−0.8	6.3	
MBD	4.3	−1.1	5.5	

provides similar accuracy with a MARE of 2.0%. When combining the same vdW methods with DFTB3, we find that crystal volumes are systematically contracted compared with the PBE+vdW methods, as can be seen from mean of volume errors in Table 1 (also can be seen in Figure 2b). The resulting

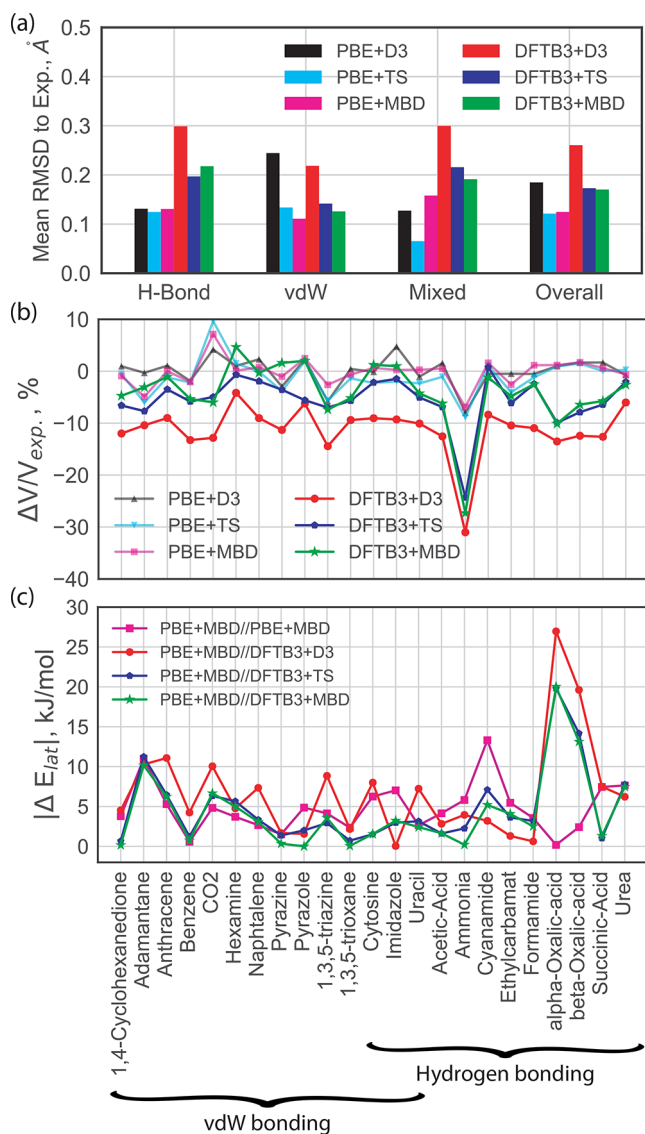


**Figure 2.** X23 benchmark data set: (a) Mean of RMSD values as calculated with respect to experimental geometries, (b) relative error of volumes with respect to experimental geometries, and (c) absolute error of lattice energies (in  $\text{kJ mol}^{-1}$ ), both with respect to the experimental values. For comparison of PBE+vdW//DFTB3+vdW combination with respect to the PBE+vdW energies, see Figure S3. We use the following abbreviations: “level of theory for energy evaluation”//“level of theory for geometry optimization”.

relative errors of 5.6 and 5.0% with respect to experiment for the DFTB3+TS and DFTB3+MBD methods dominantly originate from a strong underestimation of the volume of ammonia and the three organic acid crystals in the X23 set (vide infra), whereas the DFTB3+D3 method yields a systematic volume underestimation across the data set and an over five-fold increase in relative error of 11.2% compared with experiment. This observed volume contraction persists across the vdW-inclusive methods and partly appears to originate in

the description of Pauli repulsion in the 3ob parametrization of DFTB. The 3ob parametrization has been developed to correct the known overbinding of covalent bonds in the MIO basis set; however, intermolecular distances still seem to suffer from insufficient Pauli repulsion at longer distances. This issue is known to originate from the underlying basis confinement.<sup>27</sup>

When combined with DFTB3, TS and MBD significantly outperform D3 in their description of crystal volume. One can attribute this two-fold difference in relative error to the fitting of damping parameters of D3 in favor of energetics<sup>30</sup> rather than geometries as opposed to the optimally tuned range-separation parameters based on energetics and geometries adopted for DFTB3+TS/MBD. For the sake of comparison, we revisited the D3 range-separation parameter of D3 for DFTB3+D3(3ob) based on a balanced description of energetics and geometries (i.e., S66x8,<sup>47,48</sup> similar to TS/MBD). We find a reduced volume MARE of 8.2%, which still corresponds to a larger underestimation of crystal volumes than found with DFTB3+TS/MBD.

A few systems in the X23 set, specifically  $\text{CO}_2$  and ammonia, are persistently described poorer than others regardless of the choice of dispersion method. PBE+vdW methods fail to give reasonable volumes for  $\text{CO}_2$  and ammonia. The volume of the former is overestimated, while the latter is underestimated by 8–10%.<sup>39,49</sup> When moving from DFT to DFTB, this error becomes larger regardless of the employed method for the dispersion energy. In the case of the relatively strongly H-bonded ammonia, it is indeed more relevant to compare the optimized structure with the cubic deuterated ammonia ( $\text{ND}_3$ ) geometry at 2 K (with 128.6 versus 135.1  $\text{\AA}^3$  for ammonia at 180 K), as isotope effects can be neglected at very low temperature.<sup>10</sup> Also, organic acid groups, that is, oxalic and succinic acids, are still poorly described due to an insufficient description of charge polarization within the carboxyl groups in the 3ob parametrization.<sup>22,27</sup> These systems represent particular challenges for future parametrization work, whereas larger crystals are described consistently better with already existing parametrizations.

Contrary to the modest description of crystal volume, the internal orientation and conformation of molecular crystals is described well by DFTB3+vdW methods, as shown by RMSD errors in Figure 2a. TS/MBD yields geometries with substantially lower RMSD than D3 when compared with experimental crystal structures (0.1 Å for predominantly vdW-bound crystals and 0.2 Å for other systems). The enhanced treatment of geometries by DFTB3+TS/MBD methods combined with their significant speedup, compared with their DFT counterpart, can be advantageous in exhaustive structural search in material science. In contrast with the  $N^3$  scaling of generalized gradient approximation (GGA) functionals like PBE, DFTB scales as  $N \log(N)$  in sufficiently sparse systems.<sup>50</sup> Our performance analysis on selected X23 crystals shows that a speedup of up to a factor of 3000 can be achieved for DFTB3+TS compared with all-electron PBE+TS in FHI-aims (tight basis set),<sup>51</sup> whereas the performance gain for DFTB3+MBD is more moderate with a speed up of only 100 times. This essentially suggests that DFTB3+TS/MBD methods are optimally suited for the study of large complex molecular crystals, while smaller systems, such as the ammonia crystal, can be well treated by accurate DFT+vdW methods.

Turning to the description of lattice energies and crystal stability for the X23 data set, we find PBE+vdW methods to yield relative errors of 5.6, 6.4, and 17.5% for PBE+D3, PBE

+MBD, and PBE+TS, respectively (see Table 1 and Figure S2). The comparably large error for PBE+TS compared with PBE+D3 might seem surprising, considering that both methods describe the dispersion energy using a pairwise approximation. However, range separation or damping parameters in vdW methods can be chosen such that interaction energies for a broad range of systems are optimized. This can lead to incorporation of contributions, which at this pairwise level of treatment should not be included and could potentially negatively affect transferability across different systems. TS van der Waals functional, on the contrary, is based on free atom reference data with functional-specific range-separation tuned to exclusively represent interaction energies of small intermolecular complexes (S22), which minimizes effects beyond pairwise contributions.<sup>39</sup>

When replacing PBE+vdW with DFTB3+vdW in the description of lattice energies, regardless of vdW method, we find lattice energies with minimum MARE as high as 15% corresponding to minimum MAE of 13 kJ mol<sup>-1</sup> compared with experiment (see second column in Figure S2a of the SI). While this may disqualify the DFTB3+vdW methods in their current formulation as outright stability prediction methods, following the scheme of Figure 1, we can use the higher quality of crystal structure prediction at the DFTB3+vdW level to perform structural prescreening. Thereby, we identify stable structures using DFTB3+vdW and evaluate improved energetics at the DFT+vdW level. (We use the following abbreviations: “level of theory for energy evaluation”//“level of theory for geometry optimization”). The evaluation of lattice energies at the DFT level, that is, PBE+MBD on top of DFTB3+MBD structures, improves the lattice energy prediction significantly, as shown in Table 1 and Figure 2c. In fact, the relative error of PBE+MBD//DFTB3+TS/MBD energies is comparable in performance with the full DFT+MBD, that is, PBE+MBD//PBE+MBD when compared with experiment. This means that replacing optimized PBE+MBD crystal structures with DFTB3+TS/MBD structures does not significantly affect the lattice energy prediction compared with experiment.

Encouraged by these results, we proceed to study two highly polymorphic systems. First, we focus on coumarin with five experimentally observed polymorphs (see the inset of Figure 1), which have been recently studied by vdW-inclusive DFT.<sup>11</sup> The structures of all coumarin polymorphs have been refined at room temperature, and low-temperature structures (90 K) are available for polymorphs I, III, and IV.<sup>11</sup>

Figure 3a,b shows the RMSD results for crystal structures calculated with respect to experiment at 300 and 90 K, respectively. PBE+vdW methods yield equally good performance with a mean RMSD of just below 0.2 Å (room temperature) and 0.1 Å at 90 K. DFTB3+TS/MBD yields geometries as good as PBE+vdW with RMSD of just above 0.1 Å at 90 K. Figure 3c shows the optimized unit-cell volumes of coumarin polymorphs with respect to experimental structures. PBE+vdW methods slightly overestimate the crystal volume, whereas DFTB3+D3 strongly underestimates by >10% compared with experiment. DFTB3+TS/MBD methods provide an average relative volume error with respect to the experiment of 4.8 and 4.2%, respectively. The larger relative volume error of polymorph V, compared with other polymorphs, is due to comparison with an experimental structure measured at 300 K. This example highlights the

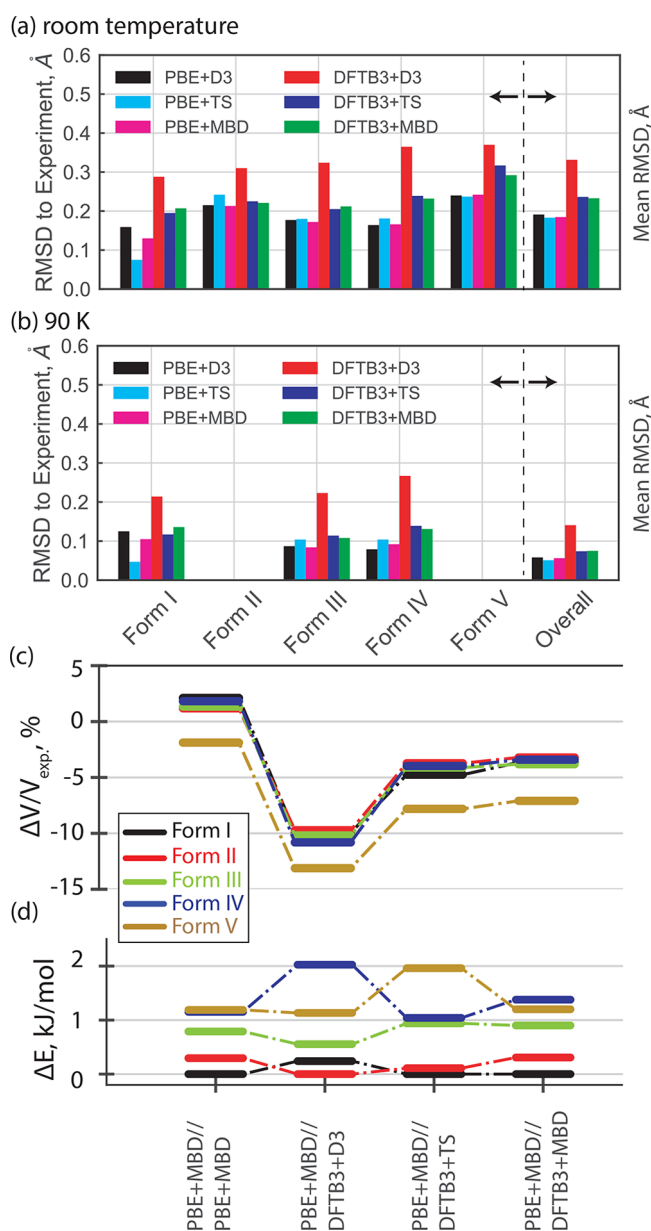


**Figure 3.** Comparison of DFT(B3)+vdW methods for coumarin polymorphs in terms of: (a) RMSD with respect to experimental structures at room temperature, (b) RMSD with respect to experimental structures 90 K (complete experimental data were not available for Forms II and V), (c) optimized unit-cell volumes  $\Delta V/V_{\text{exp}}$  in % in which 90 K experimental structures were used for comparison (except for polymorph V with structure at room temperature), and (d) stability rankings based on lattice energies  $\Delta E$  in kJ mol<sup>-1</sup>.

significant impact of thermal expansion, which is up to 4% between 300 and 90 K.<sup>11</sup>

We compare the stability rankings of coumarin polymorphs based on lattice energies, as shown in Figure 3d. Figure S6a shows the stability rankings based on DFTB3+vdW energies. It can be seen that generally they are not sufficient for accurate energy determination of polymorphic systems, although DFTB3+MBD//DFTB3+MBD captures the first two polymorphs correctly. As established herein we calculate PBE+MBD energies on top of DFTB3+vdW geometries. Experiment guides the stability rankings of coumarin forms as Form I < Form II < Form III < Form IV < Form V, with the Form I

being the most stable phase. It is quite encouraging that the full PBE+MBD and PBE+MBD//DFTB3+MBD both yield the correct energy ranking for the first three polymorphs, considering the narrow energy range within which the five polymorphs are ranked. Notice that the geometry used for final polymorph stability ranking has an impact of up to 1 kJ mol<sup>-1</sup> per molecule, see for example how the stability ranking of Form IV and V coumarin polymorphs changes between PBE+MBD//DFTB3+D3 and PBE+MBD//DFTB3+TS methods as shown in Figure 3d, which is large enough to qualitatively affect the polymorphic energy landscape.

We further extend the applicability of the methods by studying the C<sub>21</sub>H<sub>17</sub>Cl<sub>2</sub>NO<sub>2</sub> molecule from the sixth CCDC CSP blind test (molecule XXIII)—a former drug candidate molecule with five known crystalline polymorphs (see the optimized structures in Figure S4).<sup>4</sup> The preliminary results for XXIII's five known stable structures are shown in Figure S5. While all methods systematically underestimate the volumes, we show that the structures of polymorphs are best described by DFTB3+MBD with MARE of 4% with regard to experimental geometries close to full PBE+MBD calculations with MARE of 1.9% (see Figure S5a). The stability rankings of XXIII polymorphs are shown in Figure S5b (see Figure S6b for the evaluation of stability rankings based on DFT(B3)+vdW energies). We notice that the polymorphic energy landscape for flexible pharmaceutical molecular crystals is strongly dependent on the optimized geometry. Using less accurate DFTB3+D3 geometries, that is, large volume underestimations (see Figure S5a), for the final energy ranking can lead to changes of 10 kJ mol<sup>-1</sup> per molecule in the polymorphic energy differences (see Figure S5b). We observe that PBE+MBD//DFTB3+MBD ranks the first two polymorphs equal to the full PBE+MBD calculation. This is an encouraging result, which suggests that crystal structures obtained with DFTB3+vdW are more accurate when vdW interactions play a prominent role in intermolecular interactions as compared with hydrogen bonds. Because vdW interactions become most prominent in the case of flexible molecules, we anticipate vdW-inclusive DFTB to become a valuable structural prescreening tool for molecular crystals, supramolecular complexes, and systems of biological interest.

In summary, we coupled pairwise dispersion corrections and the many-body dispersion method with DFTB3 using charge population analysis and optimally tuned range-separation parameters for the current state-of-the-art 3ob parameter set for organic molecules. We examined the applicability of this approach for organic crystals using the X23 benchmark set of molecular crystals and two highly polymorphic systems, finding encouraging results. The proposed method yields significantly improved geometries compared with bare DFTB, whereas energetics can still be improved.<sup>52</sup> We suggest to improve the lattice energy prediction by calculating single-point PBE+MBD energies on top of DFTB3+vdW geometries, which were found to be very close to the full DFT calculations. We identified remaining issues in the DFTB description potentially stemming from the parametrization of the 3ob parameter set. As more suitable DFTB parametrizations become available, the here-presented approach will become even more effective for complex molecular materials. Further studies are necessary to confirm the transferability of our results to other systems, such as carbon nanostructures, larger flexible molecules, and hybrid organic–inorganic materials. Additionally, applications beyond structure search, such as the calculation of thermal corrections

and phonon spectra,<sup>53</sup> are an important field with the urgent need of efficient electronic structure methods such as the ones presented here.

## ■ COMPUTATIONAL DETAILS

We have interfaced previously published modules for the TS<sup>33</sup> and MBD<sup>34</sup> methods with the latest development version of the DFTB+ code.<sup>50</sup> DFTB3+D3/TS/MBD calculations were performed using DFTB+ and the 3ob parametrization.<sup>27</sup> We have optimized specific damping parameters for the TS/MBD methods using S66x8 dissociation curves<sup>47,48</sup> balancing the accuracy of intermolecular geometries and energies at the same time (see Figure S6 for the fitting procedure). The optimized damping parameters are 1.05 (the  $s_R$  parameter) for TS and 1.0 (the  $\beta$  parameter) for MBD. All geometry optimizations were done using the FIRE algorithm<sup>54</sup> in the Atomic Simulation Environment.<sup>55,56</sup> Root-mean-squared deviation was calculated by constructing a 15-molecule supercell, followed by a calculation of the RMSD15 value, as implemented in the Mercury package.<sup>57</sup> For RMSD calculations, only heavy atom positions were considered (hydrogen positions were ignored). DFT calculations were performed using the FHI-aims code<sup>51</sup> with PBE functional<sup>58</sup> together with D3/TS/MBD dispersion interactions. For all DFT calculations, the light basis set in FHI-aims was used for optimization and energies were obtained with the converged tight basis using the optimized structures. The automatic k-points mesh for sampling the Brillouin zone was selected such that  $n_i \times a_i = 30 \text{ \AA}$ , where  $n_i$  is the k-points sampling for the corresponding  $a_i$  lattice parameter.

## ■ ASSOCIATED CONTENT

### 📄 Supporting Information

The Supporting Information is available free of charge on the ACS Publications website at DOI: 10.1021/acs.jpcllett.7b03234.

Additional supporting data and detailed tabulations of calculated lattice volumes and energies as well as details concerning the fitting procedure for the range-separation parameters and further computational details. (PDF)

## ■ AUTHOR INFORMATION

### Corresponding Authors

\*R.J.M.: E-mail: r.maurer@warwick.ac.uk.

\*A.T.: E-mail: alexandre.tkatchenko@uni.lu.

### ORCID

Majid Mortazavi: 0000-0002-2944-7338

Jan Gerit Brandenburg: 0000-0002-9219-2948

Reinhard J. Maurer: 0000-0002-3004-785X

Alexandre Tkatchenko: 0000-0002-1012-4854

### Notes

The authors declare no competing financial interest.

## ■ ACKNOWLEDGMENTS

M.M. thanks Johannes Hoja (U Luxembourg) and R.J.M. thanks Balint Aradi (U Bremen) for fruitful discussions. J.G.B. acknowledges support by the Alexander von Humboldt foundation within the Feodor-Lynen program. M.M. and A.T. acknowledge support from the DFG SPP-1807 network. A.T. was supported by the European Research Council (ERC-CoG BeStMo).

## REFERENCES

- (1) Price, S. L.; Reutz-Edens, S. M. The potential of computed crystal energy landscapes to aid solid-form development. *Drug Discovery Today* **2016**, *21*, 912–923.
- (2) Dimitrakopoulos, C. D.; Malenfant, P. R. Organic thin film transistors for large area electronics. *Adv. Mater.* **2002**, *14*, 99–117.
- (3) Mei, J.; Leung, N. L.; Kwok, R. T.; Lam, J. W.; Tang, B. Z. Aggregation-induced emission: together we shine, united we soar! *Chem. Rev.* **2015**, *115*, 11718–11940.
- (4) Reilly, A. M.; et al. Report on the sixth blind test of organic crystal structure prediction methods. *Acta Crystallogr., Sect. B: Struct. Sci., Cryst. Eng. Mater.* **2016**, *72*, 439–459.
- (5) Cruz-Cabeza, A. J.; Reutz-Edens, S. M.; Bernstein, J. Facts and fictions about polymorphism. *Chem. Soc. Rev.* **2015**, *44*, 8619–8635.
- (6) Sun, C. C. Cocrystallization for successful drug delivery. *Expert Opin. Drug Delivery* **2013**, *10*, 201–213.
- (7) Pulido, A.; Chen, L.; Kaczorowski, T.; Holden, D.; Little, M. A.; Chong, S. Y.; Slater, B. J.; McMahon, D. P.; Bonillo, B.; Stackhouse, C. J.; et al. Functional materials discovery using energy–structure–function maps. *Nature* **2017**, *543*, 657–664.
- (8) Price, S. L. Predicting Crystal Structures of Organic Compounds. *Chem. Soc. Rev.* **2014**, *43*, 2098–2111.
- (9) Neumann, M. A.; Leusen, F. J. J.; Kendrick, J. A major advance in crystal structure prediction. *Angew. Chem., Int. Ed.* **2008**, *47*, 2427–2430.
- (10) Hoja, J.; Reilly, A. M.; Tkatchenko, A. First-principles modeling of molecular crystals: structures and stabilities, temperature and pressure. *Wiley Interdisciplinary Reviews: Computational Molecular Science* **2017**, *7*, e1294.
- (11) Shtukenberg, A. G.; Zhu, Q.; Carter, D. J.; Vogt, L.; Hoja, J.; Schneider, E.; Song, H.; Pokroy, B.; Polishchuk, I.; Tkatchenko, A.; et al. Powder diffraction and crystal structure prediction identify four new coumarin polymorphs. *Chem. Sci.* **2017**, *8*, 4926–4940.
- (12) Klimeš, J.; Michaelides, A. Perspective: Advances and challenges in treating van der Waals dispersion forces in density functional theory. *J. Chem. Phys.* **2012**, *137*, 120901.
- (13) Grimme, S.; Hansen, A.; Brandenburg, J. G.; Bannwarth, C. Dispersion-Corrected Mean-Field Electronic Structure Methods. *Chem. Rev.* **2016**, *116*, 5105–5154.
- (14) Beran, G. J. O. Modeling Polymorphic Molecular Crystals with Electronic Structure Theory. *Chem. Rev.* **2016**, *116*, 5567–5613.
- (15) Hermann, J.; DiStasio, R. A., Jr; Tkatchenko, A. First-Principles Models for van der Waals Interactions in Molecules and Materials: Concepts, Theory, and Applications. *Chem. Rev.* **2017**, *117*, 4714–4758.
- (16) Marom, N.; DiStasio, R. A.; Atalla, V.; Levchenko, S.; Reilly, A. M.; Chelikowsky, J. R.; Leiserowitz, L.; Tkatchenko, A. Many-Body Dispersion Interactions in Molecular Crystal Polymorphism. *Angew. Chem., Int. Ed.* **2013**, *52*, 6629–6632.
- (17) Reilly, A. M.; Tkatchenko, A. Role of dispersion interactions in the polymorphism and entropic stabilization of the aspirin crystal. *Phys. Rev. Lett.* **2014**, *113*, 055701.
- (18) Brandenburg, J. G.; Grimme, S. Organic crystal polymorphism: A benchmark for dispersion corrected mean field electronic structure methods. *Acta Crystallogr., Sect. B: Struct. Sci., Cryst. Eng. Mater.* **2016**, *72*, 502–513.
- (19) Whittleton, S. R.; Otero-de-la Roza, A.; Johnson, E. R. Exchange-Hole Dipole Dispersion Model for Accurate Energy Ranking in Molecular Crystal Structure Prediction. *J. Chem. Theory Comput.* **2017**, *13*, 441–450.
- (20) Al-Hamdani, Y. S.; Rossi, M.; Alfe, D.; Tsatsoulis, T.; Ramberger, B.; Brandenburg, J. G.; Zen, A.; Kresse, G.; Gruneis, A.; Tkatchenko, A.; et al. Properties of the water to boron nitride interaction: From zero to two dimensions with benchmark accuracy. *J. Chem. Phys.* **2017**, *147*, 044710.
- (21) Christensen, A. S.; Kubař, T.; Cui, Q.; Elstner, M. Semiempirical Quantum Mechanical Methods for Noncovalent Interactions for Chemical and Biochemical Applications. *Chem. Rev.* **2016**, *116*, 5301–5337.
- (22) Akimov, A. V.; Prezhdo, O. V. Large-scale computations in chemistry: a bird's eye view of a vibrant field. *Chem. Rev.* **2015**, *115*, 5797–5890.
- (23) Grimme, S.; Bannwarth, C.; Shushkov, P. A Robust and Accurate Tight-Binding Quantum Chemical Method for Structures, Vibrational Frequencies, and Noncovalent Interactions of Large Molecular Systems Parametrized for All spd-Block Elements (Z = 1–86). *J. Chem. Theory Comput.* **2017**, *13*, 1989–2009.
- (24) Elstner, M. The SCC-DFTB method and its application to biological systems. *Theor. Chem. Acc.* **2006**, *116*, 316–325.
- (25) Gaus, M.; Cui, Q.; Elstner, M. DFTB3: extension of the self-consistent-charge density-functional tight-binding method (SCC-DFTB). *J. Chem. Theory Comput.* **2011**, *7*, 931–948.
- (26) Řezáč, J. Empirical Self-Consistent Correction for the Description of Hydrogen Bonds in DFTB3. *J. Chem. Theory Comput.* **2017**, *13*, 4804–4817.
- (27) Gaus, M.; Goez, A.; Elstner, M. Parametrization and benchmark of DFTB3 for organic molecules. *J. Chem. Theory Comput.* **2013**, *9*, 338–354.
- (28) Miriyala, V. M.; Řezáč, J. Description of non-covalent interactions in SCC-DFTB methods. *J. Comput. Chem.* **2017**, *38*, 688–697.
- (29) Elstner, M.; Hobza, P.; Frauenheim, T.; Suhai, S.; Kaxiras, E. Hydrogen bonding and stacking interactions of nucleic acid base pairs: A density-functional-theory based treatment. *J. Chem. Phys.* **2001**, *114*, 5149–5155.
- (30) Brandenburg, J. G.; Grimme, S. Accurate modeling of organic molecular crystals by dispersion-corrected density functional tight binding (DFTB). *J. Phys. Chem. Lett.* **2014**, *5*, 1785–1789.
- (31) Petraglia, R.; Steinmann, S. N.; Corminboeuf, C. A fast charge-Dependent atom-pairwise dispersion correction for DFTB3. *Int. J. Quantum Chem.* **2015**, *115*, 1265–1272.
- (32) Grimme, S.; Antony, J.; Ehrlich, S.; Krieg, H. A consistent and accurate ab initio parametrization of density functional dispersion correction (DFT-D) for the 94 elements H–Pu. *J. Chem. Phys.* **2010**, *132*, 154104.
- (33) Tkatchenko, A.; Scheffler, M. Accurate molecular van der Waals interactions from ground-state electron density and free-atom reference data. *Phys. Rev. Lett.* **2009**, *102*, 073005.
- (34) Tkatchenko, A.; DiStasio, R. A., Jr; Car, R.; Scheffler, M. Accurate and efficient method for many-body van der Waals interactions. *Phys. Rev. Lett.* **2012**, *108*, 236402.
- (35) Stöhr, M.; Michelitsch, G. S.; Tully, J. C.; Reuter, K.; Maurer, R. J. Communication: Charge-population based dispersion interactions for molecules and materials. *J. Chem. Phys.* **2016**, *144*, 151101.
- (36) Markovich, T.; Blood-Forsythe, M. A.; Rappoport, D.; Kim, D.; Aspuru-Guzik, A. Calibration of the Many-Body Dispersion Range-Separation Parameter. **2016**, arXiv:1605.04987. arXiv.org e-Print archive. <https://arxiv.org/abs/1605.04987>.
- (37) Blood-Forsythe, M. A.; Markovich, T.; DiStasio, R. A.; Car, R.; Aspuru-Guzik, A. Analytical nuclear gradients for the range-separated many-body dispersion model of noncovalent interactions. *Chem. Sci.* **2016**, *7*, 1712–1728.
- (38) Otero-De-La-Roza, A.; Johnson, E. R. A benchmark for non-covalent interactions in solids. *J. Chem. Phys.* **2012**, *137*, 054103.
- (39) Reilly, A. M.; Tkatchenko, A. Understanding the role of vibrations, exact exchange, and many-body van der Waals interactions in the cohesive properties of molecular crystals. *J. Chem. Phys.* **2013**, *139*, 024705.
- (40) Yang, J.; Hu, W.; Usvyat, D.; Matthews, D.; Schütz, M.; Chan, G. K.-L. Ab initio determination of the crystalline benzene lattice energy to sub-kilojoule/mol accuracy. *Science* **2014**, *345*, 640–643.
- (41) Roux, M. V.; Temprado, M.; Chickos, J. S.; Nagano, Y. Critically evaluated thermochemical properties of polycyclic aromatic hydrocarbons. *J. Phys. Chem. Ref. Data* **2008**, *37*, 1855–1996.
- (42) Emel'yanenko, V. N.; Zaitsau, D. H.; Shoifet, E.; Meurer, F.; Verevkin, S. P.; Schick, C.; Held, C. Benchmark thermochemistry for biologically relevant adenine and cytosine. A combined experimental and theoretical study. *J. Phys. Chem. A* **2015**, *119*, 9680–9691.

- (43) Alemán, C. The keto–amino/enol tautomerism of cytosine in aqueous solution. A theoretical study using combined discrete/self-consistent reaction field models. *Chem. Phys.* **2000**, *253*, 13–19.
- (44) Blair, S. A.; Thakkar, A. J. How many intramolecular hydrogen bonds does the oxalic acid dimer have? *Chem. Phys. Lett.* **2010**, *495*, 198–202.
- (45) Jahn, M. K.; Méndez, E.; Rajappan Nair, K.; Godfrey, P. D.; McNaughton, D.; Écija, P.; Basterretxea, F. J.; Cocinero, E. J.; Grabow, J.-U. Conformational steering in dicarboxy acids: the native structure of succinic acid. *Phys. Chem. Chem. Phys.* **2015**, *17*, 19726–19734.
- (46) Keuleers, R.; Desseyn, H.; Rousseau, B.; Van Alsenoy, C. Vibrational analysis of urea. *J. Phys. Chem. A* **1999**, *103*, 4621–4630.
- (47) Řezáč, J.; Riley, K. E.; Hobza, P. S66: A Well-balanced Database of Benchmark Interaction Energies Relevant to Biomolecular Structures. *J. Chem. Theory Comput.* **2011**, *7*, 2427.
- (48) Brauer, B.; Kesharwani, M. K.; Kozuch, S.; Martin, J. M. L. The S66x8 benchmark for noncovalent interactions revisited: explicitly correlated ab initio methods and density functional theory. *Phys. Chem. Chem. Phys.* **2016**, *18*, 20905–20925.
- (49) Reilly, A. M.; Tkatchenko, A. Seamless and accurate modeling of organic molecular materials. *J. Phys. Chem. Lett.* **2013**, *4*, 1028–1033.
- (50) Aradi, B.; Hourahine, B.; Frauenheim, T. DFTB+, a sparse matrix-based implementation of the DFTB method. *J. Phys. Chem. A* **2007**, *111*, 5678–5684.
- (51) Blum, V.; Gehrke, R.; Hanke, F.; Havu, P.; Havu, V.; Ren, X.; Reuter, K.; Scheffler, M. Ab initio molecular simulations with numeric atom-centered orbitals. *Comput. Phys. Commun.* **2009**, *180*, 2175–2196.
- (52) Nyman, J.; Pundyke, O. S.; Day, G. M. Accurate force fields and methods for modelling organic molecular crystals at finite temperatures. *Phys. Chem. Chem. Phys.* **2016**, *18*, 15828–15837.
- (53) Brandenburg, J. G.; Potticary, J.; Sparkes, H. A.; Price, S. L.; Hall, S. R. Thermal Expansion of Carbamazepine: Systematic Crystallographic Measurements Challenge Quantum Chemical Calculations. *J. Phys. Chem. Lett.* **2017**, *8*, 4319–4324.
- (54) Bitzek, E.; Koskinen, P.; Gähler, F.; Moseler, M.; Gumbusch, P. Structural relaxation made simple. *Phys. Rev. Lett.* **2006**, *97*, 170201.
- (55) Bahn, S. R.; Jacobsen, K. W. An object-oriented scripting interface to a legacy electronic structure code. *Comput. Sci. Eng.* **2002**, *4*, 56–66.
- (56) Hjorth Larsen, A.; Mortensen, J. J.; Blomqvist, J.; Castelli, I. E.; Christensen, R.; Dulak, M.; Friis, J.; Groves, M. N.; Hammer, B.; Hargus, C.; et al. The atomic simulation environment? a Python library for working with atoms. *J. Phys.: Condens. Matter* **2017**, *29*, 273002.
- (57) Macrae, C. F.; Bruno, I. J.; Chisholm, J. A.; Edgington, P. R.; McCabe, P.; Pidcock, E.; Rodriguez-Monge, L.; Taylor, R.; van de Streek, J.; Wood, P. A. Mercury CSD 2.0—new features for the visualization and investigation of crystal structures. *J. Appl. Crystallogr.* **2008**, *41*, 466–470.
- (58) Perdew, J. P.; Burke, K.; Ernzerhof, M. Generalized Gradient Approximation Made Simple. *Phys. Rev. Lett.* **1996**, *77*, 3865–3868.